



NUMERICAL SIMULATION ON FAILURES OF RUBBER BEARING DUE TO THE 2016 KUMAMOTO EARTHQUAKE

S. Kusuba⁽¹⁾, T. Kobayashi⁽²⁾, K. Tasaki⁽³⁾, M. Kawakami⁽⁴⁾, J. Choi⁽⁵⁾, T. Imai⁽⁶⁾, K. Ueda⁽⁷⁾

⁽¹⁾ General Manager, R & D Department, PAL Corporation, kusuba@pal.co.jp

⁽²⁾ Assistant Manager, R & D Department, PAL Corporation, kobayashi.tooru@pal.co.jp

⁽³⁾ Deputy Director, Research Institute for Infrastructure Engineering, Nippon Engineering Consultants Co., Ltd., tasaki@ne-con.co.jp

⁽⁴⁾ President, Structural Engineering Research Institute for Disaster Prevention, masahide09210715@hotmail.co.jp

⁽⁵⁾ Assistant Manager, Division of Structural Technology, West Nippon Expressway Co., Ltd., j.choi.aa@w-nexco.co.jp

⁽⁶⁾ Committee President, Technical Committee of Rubber Bearing Association, imai@mgb.gr.jp

⁽⁷⁾ Committee Member, Technical Committee of Rubber Bearing Association, ueda@mgb-gouda.co.jp

Abstract

Most of the rubber bearings of the Okirihata bridge were damaged due to the 2016 Kumamoto earthquake. Okirihata bridge is a 5-spans steel continuous non-synthetic girder bridge with the overall length of 265m and located near the Futagawa fault which was the epicenter of the Kumamoto earthquake. By the results of field investigation conducted immediately after the disaster, it has been found that almost of the rubber parts were failed at the rubber bearings of the abutment and on the other hand, the mounting bolts were failed at the pier. It is considered that such failure of the rubber bearing is mainly caused by the large displacement occurred at the abutment and piers due to the ground deformation, which is accompanying with the fault displacement.

To investigate the failure mechanism of the rubber bearings, 3D numerical simulations were performed by using Finite Element Analysis code LS-DYNA. The investigation was carried out as a part of the study of Kyushu Association for Bridge and Structural Engineering (KABSE) Kumamoto Earthquake Special Committee. The components of the rubber bearing such as rubber, internal steel plate, top and bottom sealing plate, top and bottom loading plate, shear key and mounting bolts were modeled in detail by using FE solid elements (506560 elements). In regarding to the material properties, elasto-plastic material property was assigned to the steel. And the rubber was treated as non-linear material, which was based on the material tests conducted at the Yoshida Laboratory of the University of Yamanashi. In concerning with the load conditions, the dead load of the bridge superstructure was applied to the rubber bearing in the vertical direction. And the horizontal pushover displacements due to ground motion was applied at the top loading plate. The direction and the quantity of the pushover displacements were decided on the results of seismic response FE analysis using the whole bridge model.

As a result of simulation, it is found that the rubber bearings of both abutment and pier will be failed when shear strain of the rubber bearing exceed about 300-350%. In the case of rubber bearing at the abutment, high tensile stress concentration is observed at the bonded boundary between the rubber and the sealing plate, and this high tensile stress area will be the starting point for rubber to fail. On the other hand, the rubber bearing at the pier, the mounting bolt is failed earlier than the rubber part. Before the shear key is working, the axial stress and shear stress on the mounting bolt are generated at the same stress level. However, after the shear key is working, the increase of shear stress is saturated, but the tensile stress increasing rapidly due to the peeling force acting on the loading plate. The cross-section of the rubber bearing is 450mm*450mm or 500mm*500mm at the abutment and 650mm*650mm at the pier, respectively. Although the cross-section of the rubber plate at the pier is larger than abutment. But the size and the number of mounting bolts (M20*8) used at both abutment and pier are the same. Therefore, the mounting bolt at pier is relatively weak in comparison with the rubber part, and it will cause the mounting bolt to be failed earlier than the rubber part.

Keywords: Rubber bearing, Failure, Kumamoto Earthquake, Okirihata Bridge, Numerical Simulation, LS-DYNA



1. Introduction

Most of the rubber bearings of the Okirihata bridge were damaged due to the 2016 Kumamoto earthquake. Okirihata bridge is the 5-spans steel continuous non-synthetic girder bridge with the overall length of 265m, located near the Futagawa fault which was the epicenter of the Kumamoto earthquake.

By the results of field investigation conducted immediately after the disaster, it has been found that almost of the rubber parts were broken at the rubber bearings of the abutment and on the other hand, the mounting bolts were broken at the pier.

To investigate the failure mechanism of the rubber bearings, 3D numerical simulations were performed by using Finite Element Analysis code LS-DYNA.

This paper introduces the results of a study on estimate the failure mechanism of rubber bearings, which was carried out as part of the activities of the Kyushu Association for Bridge and Structural Engineering (KABSE) Kumamoto Earthquake Special Committee [1]. In addition, the results of preliminary studies on cyclic loading for future study are also shown.

2. Overview of Okirihata bridge

2.1 Specifications of bridge

Okirihata bridge is laying on Prefectural Road 28 (Kumamoto-Takamori line), and 5-spans steel continuous non-synthetic girder bridge with the overall length of 265m completed in 2001. Fig.1 shows the general diagram of Okirihata bridge. And Fig.2 shows the cross section of superstructure.

Route : Prefectural Road 28
(Kumamoto-Takamori line)
Length: 265m
Type : 5-spans steel continuous
non-synthetic girder bridge
Completion: 2001 (Applied Japan
specifications for highway bridges 1996)

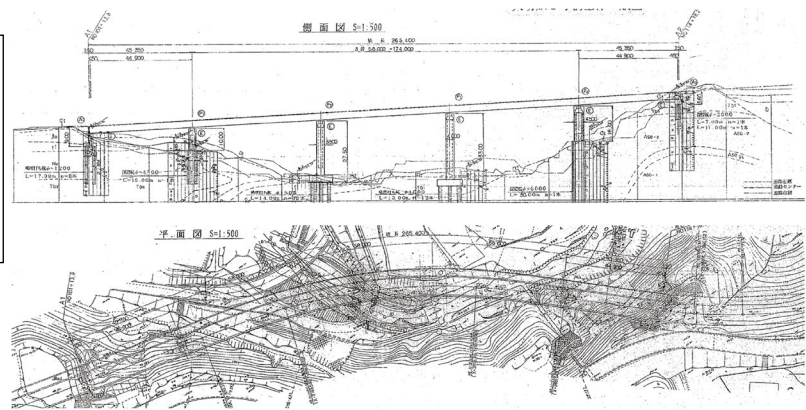


Fig. 1 – General diagram of Okirihata bridge

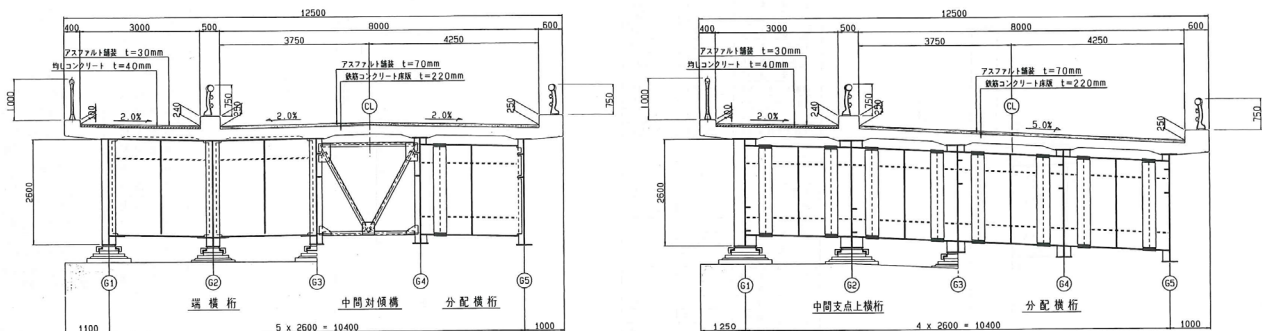


Fig. 2 – Cross section of superstructure Okirihata bridge



2.2 Specifications of rubber bearing

In this study, A1 rubber bearing was modeled as an example of the rubber bearing at abutment, and P1 rubber bearing was modeled as an example of rubber bearing at the pier. Fig.3 shows the geometry dimension of these rubber bearing. And Table 1 shows the specifications of rubber bearing.

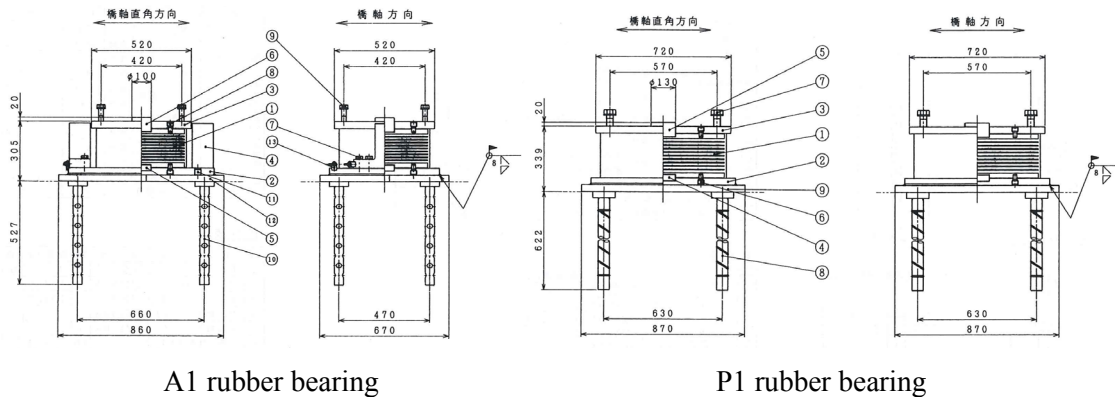


Fig. 3 – Geometry dimension of rubber bearing

Table 1 – Specifications of rubber bearing

	A1	P1
Length×Width	450mm×450mm	650mm×650mm
Rubber layers	t12mm×10 (NR-G10)	t15mm×10 (NR-G10)
Internal steel plate	t3mm×9 (SS400)	t3mm×9 (SS400)
Upper and lower sealing plate	t25mm (SM490A)	t25mm (SM490A)
Upper and lower shoe	t38mm (SM490A)	t38mm (SM490A)
Mounting bolts	M20×8 (SCM435)	M20×8 (SCM435)
S1	9.4	10.8
S2	3.8	4.3

3. Failure mode of rubber bearings

The failure mode of the rubber bearing for each abutment and pier is shown in Table 2.

In the Okirihata bridge, the rubber bearings are adopted as a structure to disperse the horizontal force during the earthquake. Therefore, the support condition is elastic support in the both longitudinal and transvers direction. A1 and A2 abutments have side blocks as joint protectors to protect the bridge joints during earthquakes below level 1 earthquake ground motion.

Fig.4 shows the failure of A1 abutment G5 bearing. In the abutments, the rubber bearing was completely broken at rubber part. Since the side blocks on both sides are also broken, it is assumed that the superstructure vibrated in the direction perpendicular to the bridge axis. Observing the fracture surface of the rubber, the fracture of the rubber is occurred at not bonding surface but in the rubber material. In addition, traces of the collision of the girders were confirmed on the parapet surface.

Fig.5 shows the failure of P4 pier G5 bearing. On the other hand, in the piers, the mounting bolts were broken on the P1, P3, and P4 piers, and main girder was displaced to the valley side from the original



position. In these rubber bearings, it is assumed that the rubber body did not break as the reason for upper mounting bolt was broken and the shear key was released.

Fig.6 shows the failure of P4 pier G1 bearing (superstructure side). Since the bolt was broken at the position protruding from the lower surface of the sole plate, it can be considered that the fracture of mounting bolt was not caused by shear force but tension force.

Fig.7 shows the failure of P2 pier G3 bearing. In this bridge, only P2 rubber bearing did not lose the horizontal force supporting function completely. But P2 rubber bearing was deformed toward the valley side with large shear deformation and crack on rubber part.

Table 2 – Failure mode of the rubber bearing for each position

Abutment, Pier	Failure mode of rubber bearing
A1	Completely broken at rubber part Broken of side blocks on both sides
P1	Broken of mounting bolts
P2	Shear deformation Cracked on rubber part
P3	Broken of mounting bolts
P4	Broken of mounting bolts
A2	Completely broken at rubber part Broken of side blocks on both sides



Fig. 4 – Failure of A1 abutment G5 bearing



Fig. 5 – Failure of P4 pier G5 bearing



Fig. 6 – Failure of P4 pier G1 bearing



Fig. 7 – Failure of P2 pier G3 bearing

4. FE analysis

As mentioned, it has been found that rubber part of the rubber bearing was broken at the abutment, on the other hand, the mounting bolt was broken at the pier. So, we try to estimate the failure mechanism of rubber bearing by reproducing the difference of failure mode between abutment and pier. The FE analysis are performed for A1 rubber bearing as an example of abutment, and P1 rubber bearing as an example of pier.



4.1 FE model

Fig.8 shows the FE model for A1 rubber bearing. And Fig.9 shows the FE model for P1 rubber bearing. The components of the rubber bearing such as rubber, internal steel plate, upper and lower shoe, upper and lower sealing plate, shear key and mounting bolts were modeled in detail by using FE hexahedral solid elements (506560 elements). The element size was based on a cubic element with a side length of 5 mm, which had decided by preliminary analysis for the best balance of accuracy, calculation time, and avoidance of element collapse due to large deformation.

Friction contact was modeled for between shear key and its surrounding steel plates, between mounting bolt and its surrounding steel plates, and between lower shoe and base plate. Here, the friction coefficient was assumed to 0.15, which is a general value of the static friction coefficient between steel and steel.

Fig.8 and Fig.9 also shows the load conditions and constraint conditions. The dead load of the bridge superstructure is loading to the upper shoe. After that, the horizontal displacement is loading gradually increased to the upper shoe (Pushover analysis). For the constraint conditions, after completely fixing the displacement of the base plate, and the displacement of the portion corresponding to the outer peripheral weld between the lower shoe and base plate was fixed.

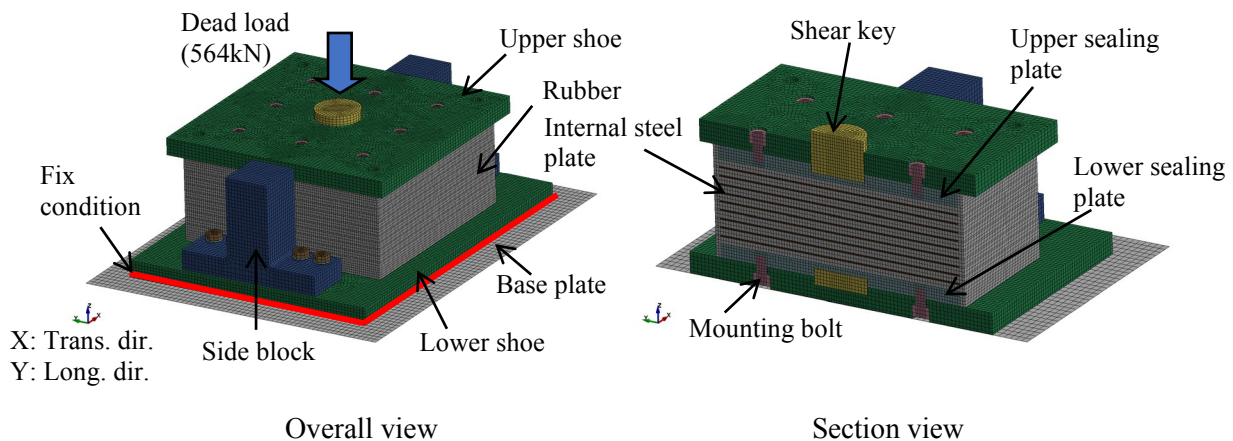


Fig. 8 –FE model for A1 rubber bearing

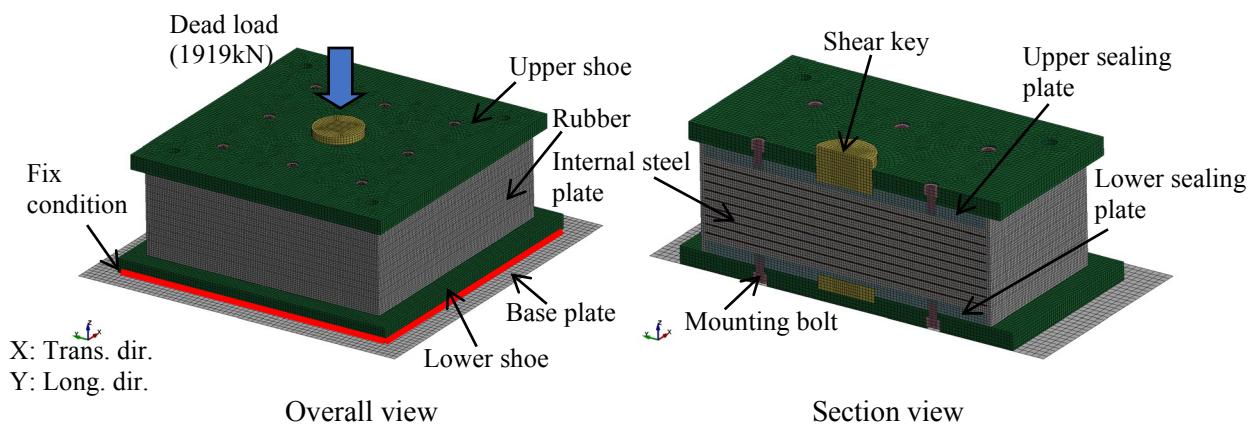


Fig. 9 –FE model for P1 rubber bearing



The direction and the quantity of the pushover displacements were decided by the results of seismic response FE analysis using the whole bridge model [1]. As an example, Fig.10 shows the time history of horizontal displacement and orbit at upper shoe for A1 abutment G2 bearing. The pushover displacement is assumed to be the displacement and direction at the time when the maximum value for horizontal resultant displacement.

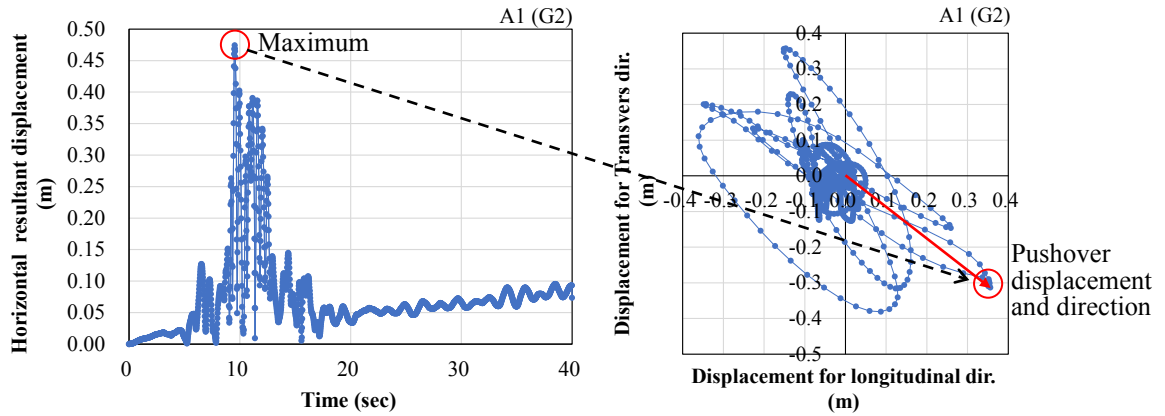


Fig. 10 – Time history of horizontal displacement and orbit (A1 abutment G2 bearing)

Table 3 shows the analysis cases and the pushover displacement for each case. A1-Long. and P1-Long. are the cases for loading to the longitudinal direction. And A1-Diag. and P1-Diag. are the cases for loading to the diagonal direction decided by the method as shown in Fig.10.

Table 3 – Failure mode of the rubber bearing for each position

Case	Location of bearing	Pushover horizontal displacement on top loading plate				Pushover rotation on top loading plate	
		Longitudinal direction (m)	Transvers direction (m)	Resultant displacement (m)	Shear Strain (%)	Around long. axis (rad.)	Around Trans. axis (rad.)
A1-Long.	A1	4.800E-01	0.0	4.800E-01	4.000E+02	0.0	0.0
A1-Diag.		3.562E-01	-3.133E-01	4.744E-01	3.953E+02	7.518E-03	-1.823E-03
P1-Long.	P1	6.000E-01	0.0	6.000E-01	4.000E+02	0.0	0.0
P1-Diag.		3.762E-01	-2.499E-01	4.516E-01	3.011E+02	1.319E-03	-3.913E-03

4.2 Superelastic model for rubber

The OGDEN model was used as the superelastic model for rubber material [2]. In this model, the strain energy density function is defined as in Eq. (1).

$$W^* = \sum_{i=1}^3 \sum_{j=1}^n \frac{\mu_j}{\alpha_j} (\lambda_i^{\alpha_j} - 1) + K(J - 1 - \ln J) \tag{1}$$

Here, μ_j and α_j are material constants.

J: Relative volume

K: Bulk modulus



The material constants were identified based on the results of a lap shear test using a cylindrical specimen performed at the Yoshida Laboratory of the University of Yamanashi [3]. Fig.11 shows the cylindrical specimen. And Fig.12 shows the relationship between shear stress and shear strain measured in the test.

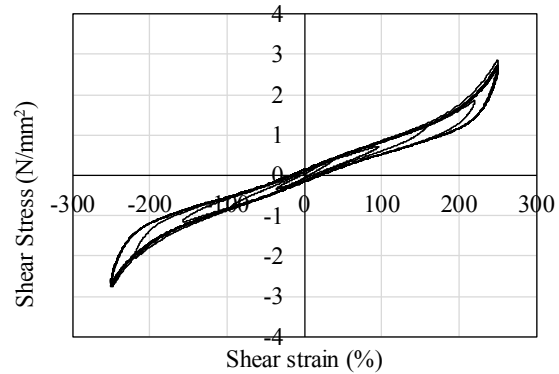
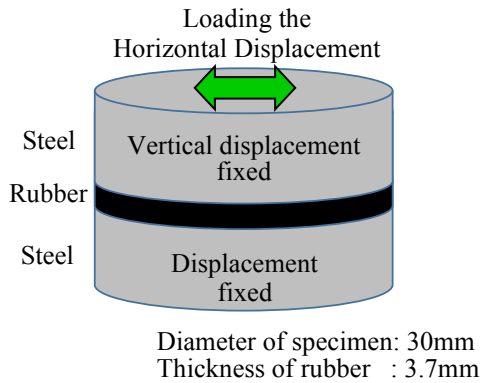


Fig. 11 – Overview of cylindrical specimen

Fig. 12 – Shear stress-strain measured in the test

The FE analysis to reproduce the lap shear test was performed. The material constants were identified by trial and error in the FE analysis. Fig.13 shows the shear stress-shear strain relationship obtained by FE analysis. Table 4 shows the material constants in Eq. (1) identified by FE analysis.

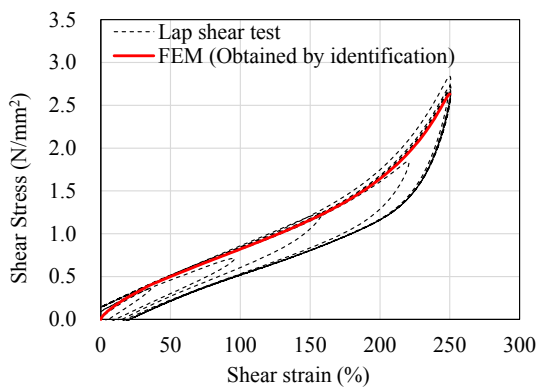


Table 4 – Material constants in Eq. (1)

J	μ_j	α_j
1	2.0	0.9
2	9.0E-4	8.0
3	-5.0E-3	-3.5

Fig. 13 – Shear stress-strain reproduced by FE analysis

4.3 Material properties of steel

Table 5 shows the material constants for steel. In the FE analysis, the elasto-plastic properties of steel materials were considered. And stress-strain relationship was treated by bilinear approximation with elastic modulus and hardening modulus.

Table 5 – Material properties of steel

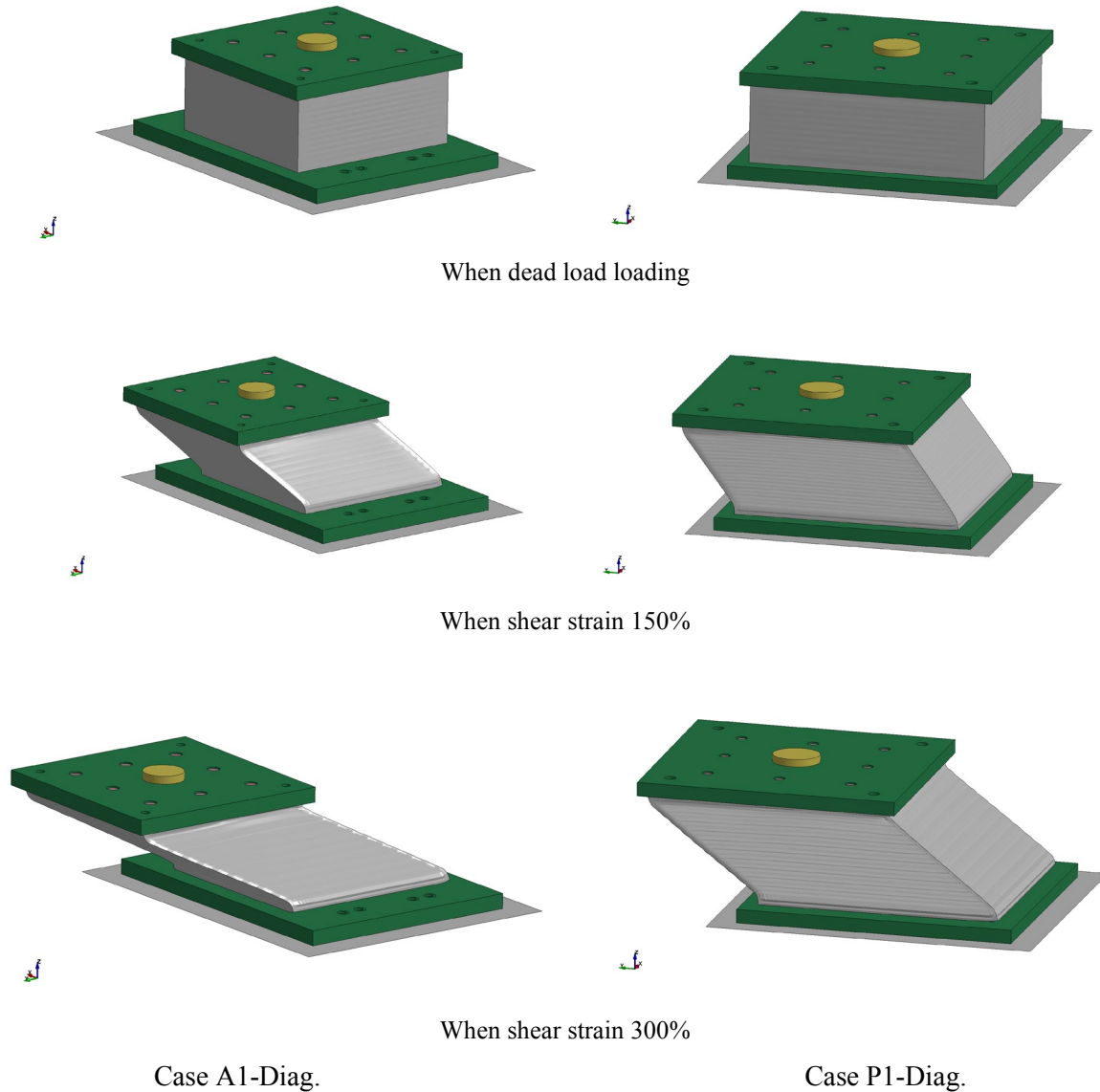
Material	Elastic modulus E (N/mm ²)	Poisson's ratio ν	Yield stress σ_y (N/mm ²)	Tensile strength σ_b (N/mm ²)	Elongation ϵ_b (mm/mm)	Hardening Modulus E'	Stress-Strain curve
SS400	206000	0.3	245	455	0.21	$(\sigma_b - \sigma_y) / (\epsilon_b - \epsilon_y)$	Bilinear approximation
SM490A			315	550	0.21		
SCM435			940	1040	0.09		



5. Analysis results

5.1 Deformation

Fig.14 shows the deformation of case A1-Diag. and case P1-Diag..



When dead load loading

When shear strain 150%

When shear strain 300%

Case A1-Diag.

Case P1-Diag.

Fig. 14 – Deformation

5.2 Shear stress-strain relationship

Fig.15 shows the shear stress-strain relationship of case A1-Diag. and case P1-Diag.. The shear stress-strain relationship is approximately equal to the shear modulus of elasticity 1.0N/mm^2 (Rubber material: NR-G10) in the range up to shear strain about 225%. And hardening occurs remarkably in the region where the strain exceeds 225%.

In the case of A1-Diag., the disturbance in the increase of stress occurs when the shear strain exceeds 300%. This time point corresponds to the timing at which the shear key begins to contact the surrounding steel sheet. It is considered that such a disturbance in the tendency of the increase of stress is due to local plasticization of the contact area and change in the contact surface. In other analysis cases, the disturbance of the stress occurs similarly.

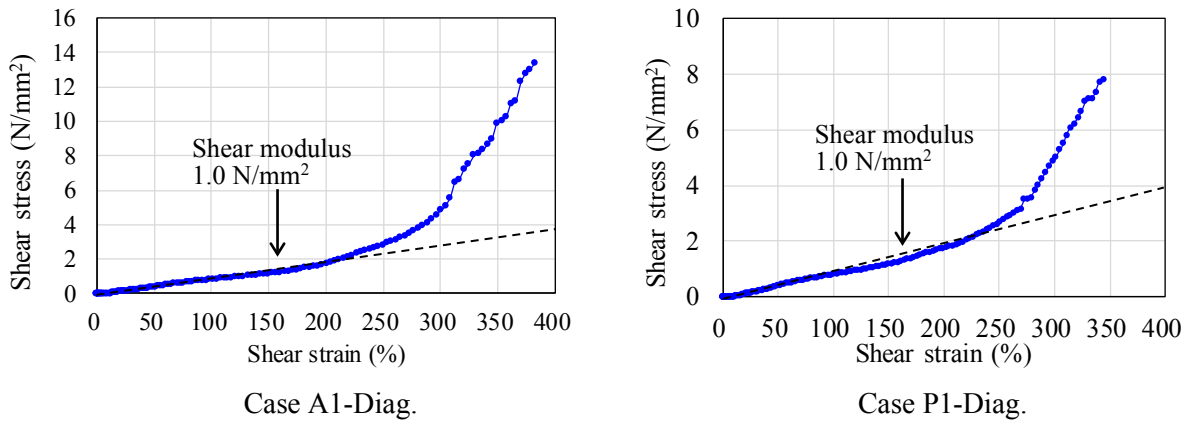


Fig. 15 – Shear stress-strain relationship

5.3 Failure criterion for rubber part

Fig.16 shows the deformation and the maximum principal stress when the shear strain 326% for case A1-Long.. The high tensile stress is generated in the rubber at the boundary between rubber part and the lower sealing steel plate (Same for upper sealing plate side). This high stress part may be the starting point of rubber breaks. This part is near the region where the compressive stress acts due to dead load. It is considered that tensile stress concentration is produced by effect of the vertical compressive restraining force due to dead load and the effect of tension field due to shear force.

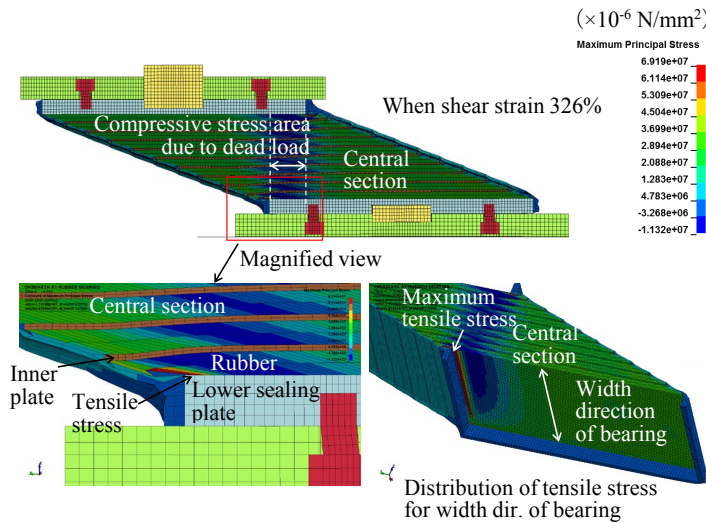


Fig. 16 – Deformation and the maximum principal stress (Case A1-Long.)

The rupture stress criterion of rubber was investigated by performed the reproduction FE analysis of the uniaxial tensile test (JIS K6251) for rubber material. Fig.17 shows the deformation and the maximum principal stress obtained by FE analysis. The tensile stress 63.1N/mm² (true stress) is adopted as the rupture stress criterion. This stress is the maximum value of the maximum principal stress in FE model when the nominal tensile stress reaches the standard tensile strength 15.0N/mm² (nominal stress).

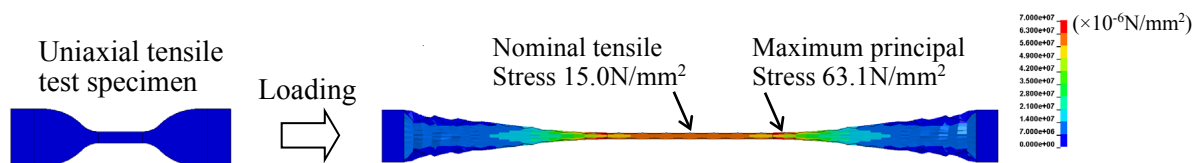


Fig. 17 – Deformation and the maximum principal stress (FE analysis for the uniaxial tensile test)



5.4 Failure criterion for mounting bolt

Eq. (2) was adopted as the bolt criterion based on the results of the bolt fracture test under the combined conditions of axial stress and shear stress [4]. It was assumed that the bolt would break when the D value is 1.0 or more.

$$D = \left(\frac{\sigma_t}{\sigma_{tf}} \right)^2 + \left(\frac{\tau_s}{\tau_{sf}} \right)^2 \quad (2)$$

Here, σ_t : Axial stress acting on bolt

τ_s : Shear stress acting on bolt

σ_{tf} : Tensile break strength = 1040N/mm²

τ_{sf} : Shear break strength = 600N/mm²

Size of mounting bolt : M20 (Effective area=245mm²)

Material (Grade) : SCM435 (10.9)

5.5 Evaluation results for rubber part and mounting bolt

Fig.18-(a) shows the relationship between the maximum value of maximum tensile stress on rubber part and the shear strain for case A1-Diag.. The tensile stress exceeds the rupture stress criterion of the rubber when the shear strain at 329%. So, the rubber may be start breaking at this timing. And, Fig.18-(b) shows the relationship between the fracture criterion D of the bolt and the shear strain. The D value did not exceed 1.0 in the range up to the shear strain 380%, where the FE analysis was performed. So, it is considered that the mounting bolt does not break.

Fig.19-(a) shows the relationship between the maximum value of maximum tensile stress on rubber part and the shear strain for case D1-Diag.. The tensile stress did not exceed the rupture stress criterion of the rubber in the range up to the shear strain 345% where the FE analysis was performed. So, it is considered that the rubber part does not break. And, Fig.19-(b) shows the relationship between the fracture criterion D of the bolt and the shear strain. The D value exceeds 1.0 when the shear strain at 304%. Therefore, it is considered that the mounting bolt may be start breaking at this timing.

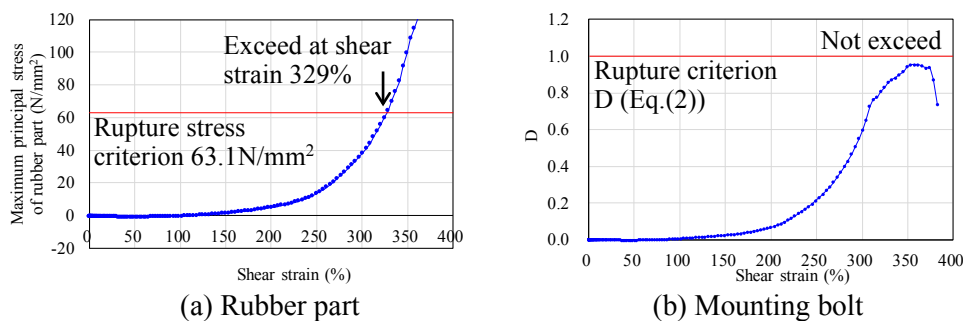


Fig. 18 – Evaluation of failure for Case A1-Diag.

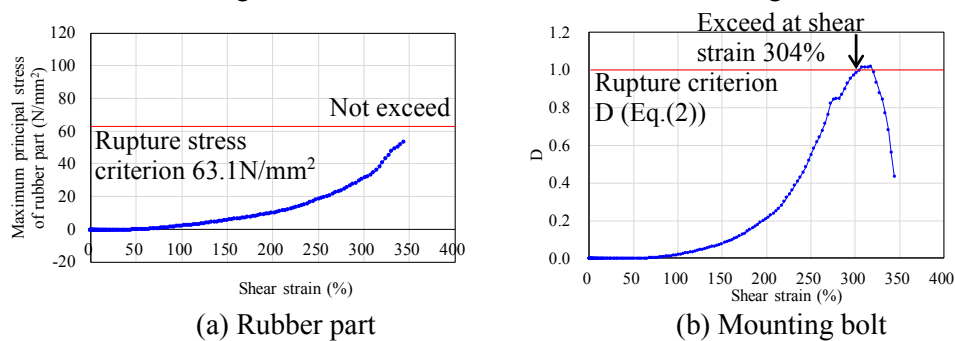


Fig. 19 – Evaluation of failure for Case P1-Diag.



Table 6 shows the result of evaluation of failure for rubber part and mounting bolt.

Table 6 – Result of evaluation of failure

Case	Location of bearing	Loading direction	Failure load (Shear strain at failure load)	The part that breaks first
A1-Long.	A1	Longitudinal	Rubber part: 1551kN (326%) Mounting bolt: over 2838kN (380%)	Rubber part
A1-Diag.		Diagonally	Rubber part: 1629kN (329%) Mounting bolt: over 2712kN (374%)	Rubber part
P1-Long.	P1	Longitudinal	Rubber part: 3291kN (338%) Mounting bolt: 2778kN (321%)	Mounting bolt
P1-Diag.		Diagonally	Rubber part: over 3298kN (345%) Mounting bolt: 2229kN (304%)	Mounting bolt

5.6 Preliminary study for cyclic loading

The FE analysis and evaluation of failure shown above are for once pushover loading condition. However, the rubber bearing of actual bridge receives cyclic loading due to earthquake ground motion and vibration of bridge. In order to carry out the FE analysis for cyclic loading, we studied on the treating of Mullins effect [5] for rubber materials.

The study on treating of the Mullins effect was performed by using the results of the lap shear test shown in Fig. 12. In the FE analysis code LS-DYNA, the Mullins effect is defined by inputting the table between the strain energy density function and the damage factor value [2].

Fig. 20 shows the results of treating on Mullins effect. The relationship between the shear stress and the shear strain for the first loading process, unloading process, and in the second and subsequent loading processes can be properly reproduced.

And also, the trial FE analysis on cyclic loading was performed for case A1-Long. The pushover displacement was applied to shear strain 200%, which is 0.8 times for the design shear strain 250%, then unloaded to 0%, and applied again to over 350%. Fig. 21 shows the comparison of tensile stress of rubber part between once loading condition and cyclic loading condition. Both results show that the rubber part may start to break at a shear strain around 325%. It was found that there was no significant difference on timing of failure of rubber part within the loading conditions in this study.

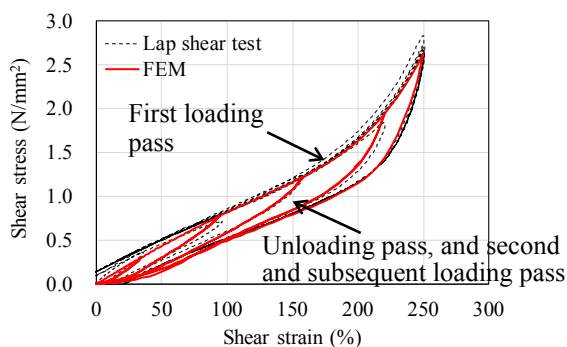


Fig. 20 – Modeling the Mullins effect

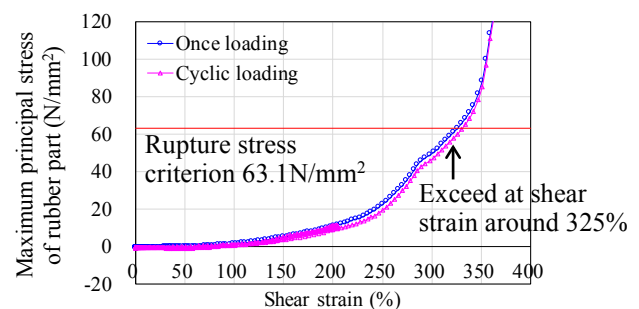


Fig. 21 – Comparison of tensile stress of rubber part

6. Conclusion

The knowledge obtained by this study are as described below.

- (1) Focusing on the difference of the failure mode, A1 (Abutment) rubber bearing has broken at the rubber part. On the other hand, the P1 (pier) rubber bearing has broken at the bearing mounting (See Table 6). These analysis results are consistent with the failure mode for the rubber bearing on the actual bridge.



- (2) In the case of A1 rubber bearing, high tensile stress is acting on the rubber part at the boundary between the rubber part and the sealing steel plate. This part may be the starting point of rubber breaks. This part is near the region where the compressive stress acts due to dead load. It is considered that tensile stress concentration is produced by effect of the vertical compressive restraining force due to dead load and the effect of tension field due to shear force.
- (3) For both A1 and P1 rubber bearings, the axial stress, shear stress and bending stress act on the mounting bolt in combination. For the shear stress, the increase of the stress value has yielded when the shear key starts to be acting by contact to the sealing plate. On the other hand, the tensile axial stress has increased rapidly after the shear key began to acting. It is considered that the main cause of the fracture of mounting bolt is the effect of this tensile axial stress.
- (4) The cross-sectional dimensions of the A1 rubber bearing are 450 mm x 450 mm, while the cross-sectional dimensions of the rubber bearing are 650 mm x 650 mm. Although the cross-sectional area of the rubber part is about twice as large for the P1 rubber bearing compared with A1, but the mounting bolts for both are the same (M20×8). So, in the case of the P1 rubber bearing, the mounting bolt will be broken first because the mounting bolt was relatively weaker than the rubber part.
- (5) In order to carry out the FE analysis for cyclic loading, we studied on the treating of Mullins effect for rubber materials. And, the trial FE analysis on cyclic loading was performed for case A1-Long. It is found that there is no significant difference between once loading and cyclic loading within the in this study.

According to the analysis results, The A1 rubber bearing has failed at the rubber part when the shear strain 329%. For the mounting bolt, the P1 rubber bearing has failed when the shear strain 304%. These strains are far larger than 250%, which is design load strain for rubber bearing level 2 earthquake ground motion. The ground motion level of the 2016 Kumamoto earthquake is not higher than the level 2 earthquake ground motion [6]. So, it is probable that the damage of rubber bearing was greatly affected by ground deformation due to fault rupture.

In order to prepare for the occurrence of an unexpected level earthquake, it is necessary to understand the 'limit state of rubber bearing' in detail. For this purpose, it is necessary to conduct an experiment to verify the performance of rubber bearings under all conditions and all specifications. So, the FE analysis is useful to evaluate the performance of rubber bearings for complex behavior of earthquake.

In the FE analysis, it is important to identify the superelastic model of the rubber material and detailed modeling of the rubber bearing components. In order to improve the accuracy of analysis, it is necessary to create a database of the superelastic model by conducting rubber material tests and improvement of the modeling method.

7. References

- [1] Kyushu Association for Bridge and Structural Engineering (KABSE) (2019): 2016nen Kumamotojishin Higaichousa Bunseki Houkokusho (The report of the 2016 Kumamoto earthquake damage investigation and analysis)
- [2] LS-DYNA KEYWORD USER'S MANUAL VOLUME II Material Models, LSTC
- [3] Narita Hiromichi (2019): Zairyoshiken Database no tameno Kyoryoyou Menshingomu no Tajikurikigakutokusei no Haaku (Understanding multi-axial mechanical properties of seismic isolation rubber for bridges for material testing database), Bachelor thesis of Faculty of Engineering of the University of Yamanashi
- [4] Hashimoto Atsuhide, Yamada Tomohisa (1992): Ultimate Shear Strength of High Strength Bolts, *Journal of Structural and Construction Engineering*, No 440, Architectural Institute of Japan
- [5] L. Mullins (1948): Effect of Stretching on the Properties of Rubber, *Rubber Chemistry and Technology*, June 1948, Vol. 21, No. 2, pp. 281-300.
- [6] Japan Society of Civil Engineers - west (2019): Heisei 28nen Kumamotojishin Higaichousa Houkokusho (The report of the 2016 Kumamoto earthquake damage investigation), http://jsce.or.jp/branch/seibu/00_active/, ref. 2019